Acta Pharm. **75** (2025) 613–628
https://doi.org/10.2478/acph-2025-0031

Original research paper

Antioxidant activity of methyl caffeate: Evidence of proton-coupled electron transfer reaction mechanism

ANA KARKOVIĆ MARKOVIĆ*
VIKTOR PILEPIĆ
CVIJETA JAKOBUŠIĆ BRALA
AGNEZA RUKAVINA
ANDREA ŠTEHEC

University of Zagreb Faculty of Pharmacy and Biochemistry 10000 Zagreb, Croatia

ABSTRACT

Methyl caffeate (MC), a naturally occurring methyl ester of caffeic acid (CA), exhibits potent antioxidant activity and a broad spectrum of biological effects. This study investigates the antioxidant mechanism of MC through its reaction with the stable radical DPPH•, employing both experimental and computational approaches. Kinetic measurements were conducted in a predominantly nonpolar medium (1,4-dioxane with phosphate buffer), revealing concerted proton and electron transfer. This experimental evidence was supported by values of kinetic isotope effects (KIEs) and thermodynamic activation parameters. Analysis of the intrinsic bond orbitals (IBOs) along the calculated intrinsic reaction coordinate (IRC) trajectories supported the proposed proton-coupled electron transfer (PCET) reaction mechanism. Additionally, the Fe(II) complexation ability of MC was evaluated spectrophotometrically, demonstrating stable complex formation at pH 7.0, suggesting potential for mitigating hydroxyl radical generation in physiological conditions. These findings offer new insights into the antioxidant behaviour of MC and its potential applications in pharmaceutical and nutraceutical formulations.

Keywords: methyl caffeate, proton-coupled electron transfer, hydrogen tunnelling, kinetic isotope effect, intrinsic bond orbital analysis, Fe(II) complex

Accepted November 28, 2025
Published online November 29, 2025

INTRODUCTION

Hydroxycinnamic acids (*p*-coumaric, caffeic, ferulic, and sinapic acids) are simple phenolic acids widely distributed as secondary metabolites in the plant kingdom. They have been extensively studied due to their diverse bioactive properties (1–3). These natural compounds are commonly used in the cosmetic, food, pharmaceutical, and health industries as supplements or additives, primarily for their antioxidant and antimicrobial activities (1, 3–5).

Methyl caffeate (MC), the naturally occurring methyl ester of caffeic acid (CA) found in various plant species, also exhibits a wide range of biological activities (6–8), including anticancer (6, 8), antioxidant (6, 9–11), antidiabetic (7, 12, 13), antimicrobial (4, 14, 15), anti-inflammatory (16, 17), neuroprotective (18), antisenescence (16), among others.

* Correspondence; e-mail: ana.karkovic@pharma.unizg.hr

In a recent study on *Morus nigra* Linn. extracts, MC isolated from the fruit demonstrated remarkable inhibition of HeLa cell proliferation and migration, induced apoptosis *in vitro*, and further inhibited tumour growth in a HeLa xenograft model *in vivo*, acting as a natural 3-phosphoglycerate dehydrogenase (PHGDH) enzyme inhibitor (6). Regarding its antidiabetic effects, MC isolated from the flower of *Prunus persica* (L.) Batsch enhanced glucose-stimulated insulin secretion in INS-1 cells, in a manner similar to gliclazide, an antidiabetic sulfonylurea drug. This effect was attributed to the upregulation of proteins involved in pancreatic β-cell metabolism (7).

MC showed major antimicrobial activity against human pathogenic bacteria such as *Streptococcus mutans* and *Escherichia coli* (14) and moderate antimicrobial activity against *Proteus vulgaris*, *Klebsiella pneumoniae* and *Mycobacterium tuberculosis* (15). Poly(lactic-co-glycolic acid) (PLGA) nanoparticles loaded with MC were tested against a plant pathogenic bacteria *Ralstonia solanacearum* and showed good sustained-release properties and antibacterial effects, with potential to be an alternative to traditional pesticides (19).

Many biological activities of MC are linked to its ability to suppress or scavenge reactive oxygen species (ROS). In the study by Masuoka *et al.*, MC and other short-chain alkyl caffeates acted as effective scavengers and strong inhibitors of superoxide anion ($O_2^{\bullet-}$) generation, which is crucial in preventing the initiation of lipid peroxidation and hydroxyl radical formation. The same study also reported considerable DPPH• (2,2-diphenyl-1-picrylhydrazyl radical) scavenging activity for both CA and alkyl caffeates (10). MC has also shown significant protective effects against oxidative stress-induced neuronal cell damage by inhibiting both H_2O_2-induced caspase-3 and cathepsin D activities in neuronal-like SH-SY5Y cells (18).

As a derivative of CA, MC retains the characteristic *o*-dihydroxylbenzene (catechol) and an α,β-unsaturated side chain in its structure (Fig. 1). The presence of a methyl ester group increases its lipophilicity, thereby enhancing membrane permeability. This was demonstrated in a study by Garrido *et al.*, which showed that CA esters exhibited greater antioxidant activity and improved lipophilicity compared to CA, and consequently were able to protect PC12 neuronal cells from oxidative stress (20).

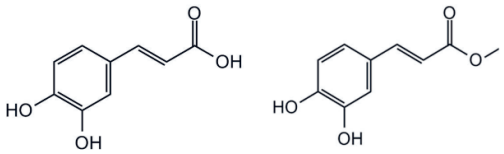

Fig. 1. Structures of caffeic acid (CA) and its methylated derivative methyl caffeate (MC).

Although the antioxidant potential of MC is well established, the mechanism underlying its action remains relatively underexplored. In general, the antioxidative activity of phenol (ArOH) could be presented by the following equations (21–23):

First step: $R\bullet + ArOH \rightarrow RH + ArO\bullet$ (*1*)

Second step: $ArO\bullet + R\bullet \rightarrow$ products (*2*)

or

$ArO\bullet + ArO\bullet \rightarrow$ dimer or disproportionation products (*3*)

in which R• is radical (for example hydroxyl HO•, peroxyl ROO•, alkoxyl RO•…), ArO• is phenoxyl radical and RH is an unreactive species. Second step reactions (Equations *2* and *3*) are irreversible and lead to non-radical products. Formal hydrogen atom transfer (transfer of electron and proton, Equation *1*) from ArOH to R• may occur *via* several different mechanisms: concerted, such as hydrogen atom transfer (HAT) or proton-coupled electron transfer (PCET), and consecutive, such as sequential proton loss electron transfer (SPLET) or single electron transfer followed by proton transfer (SET-PT), among others (22, 24, 25). The main difference between the concerted mechanisms HAT and PCET lies in the proton and electron transfer sites. In HAT, both transfers occur at the same site – typically the same atom, bond, or orbital – whereas in PCET, the proton and electron are transferred to or from different sites. Computational chemistry methods such as DFT calculations can be employed to differentiate between these mechanisms (23). HAT/PCET mechanisms are considered predominant for the reaction of ArOH and R• in nonpolar solvents, whereas SPLET is favoured in polar solvents due to enhanced dissociation of phenolic OH groups and the increased reactivity of phenolate anions (22, 24). *In silico* study of antioxidant properties of caffeic acid derivatives confirmed that HAT and SPLET pathways are thermodynamically favourable for MC, with the environment (nonpolar *vs.* polar) dictating mechanism preference, but experimental evidence for these mechanisms still lacks (24).

Another important property of phenolic compounds containing a catechol moiety is their ability to chelate transition metal ions (26, 27). Ferrous ion, in particular, catalyse the decomposition of hydrogen peroxide into hydroxyl radicals, the most reactive oxygen species, *via* the Fenton reaction (28). Fe(II) phenol complexes exhibit a characteristic band in the visible region, with absorption maxima observed in the range of 450–600 nm (29–31). Mazzone *et al.* employed DFT analysis to study various caffeic acid-based Fe(II) ligands (32).

The aim of this study was to investigate the antioxidant activity of MC in the reaction with DPPH•, by means of experimental and computational chemistry methods. DPPH• is a stable radical characterized by a strong absorption band in the visible region ($\lambda_{max} \approx 520$ nm), commonly used as a model radical for studying the reactions of phenols with peroxyl radicals, ROO•, which play a crucial role in biological systems (21, 22, 33, 34). Reactions were conducted in predominantly nonpolar medium made of 1,4-dioxane and phosphate buffer pH 5.9 or 7.2 (5 and 15 %, *V*/*V*), to explore the effects on kinetic parameters. Reaction rate constants, kinetic isotope effects, and thermodynamic activation parameters were determined both experimentally and through DFT calculations, and the PCET mechanism was proposed for the reaction between MC and DPPH•. Additionally, the Fe(II) complexation ability of MC was evaluated spectrophotometrically. Taken together, the findings of this study aim to provide a deeper insight into the antioxidant activity of MC.

EXPERIMENTAL

Reagents and chemicals

1,4-dioxane, 2,2-diphenyl-1-picrylhydrazyl (DPPH•), caffeic acid, HCl (1 mol L^{-1}, Titrisol), NaOH (1 mol L^{-1}, Titrisol), DCl (99 % D), NaOD (40 % *m*/*m*, 99.5 % D), $CDCl_3$ (> 99.8 %), H_2SO_4 (≥ 98 %), $NaHCO_3$ (≥ 99.5 %) and buffer standards pH 4 and pH 7 were obtained from

Merck, KGaA, (Germany). Methanol (≥ 99.9 %) was supplied from Honeywell (USA), ethyl acetate (> 99.5 %) was from Fluka Chemie GmbH (Switzerland), and Na_2SO_4 (≥ 99 %, anhydrous) was from Kemika (Croatia). Iron(II) sulphate heptahydrate (99+ %) was obtained from Acros Organics (Belgium), K_2HPO_4 and KH_2PO_4 from J. T. Baker (Netherlands). Water and heavy water (Sigma-Aldrich, 99.9 % D) were twice distilled and carbon dioxide- and oxygen-free (bubbled with 99.999 % N_2, Messer, Germany).

Synthesis of the methyl caffeate

MC was synthesized from CA and methanol following a previously published procedure (35). Briefly, 500 mg of CA was dissolved in 30 mL of methanol containing 1 mL of concentrated H_2SO_4, and the mixture was heated under reflux for approximately 1 hour at 65–70 °C. After cooling to room temperature, the solution was diluted with 150 mL of ethyl acetate and washed repeatedly with an aqueous solution of $NaHCO_3$ (5 %, *m*/*V*) until a neutral pH was achieved. The organic layer was subsequently washed with distilled water, dried over anhydrous Na_2SO_4, and the solvent was removed under vacuum. The identity of the synthesized compound was confirmed by ^{1}H NMR spectroscopy (Bruker Avance 600 (14.1 T) NMR spectrometer) through comparison of chemical shift values and the appearance of characteristic absorption bands with literature data (35, 36); ^{1}H-NMR (600 MHz, $CDCl_3$, δ/ppm): 7.59 (1H, d, *J* = 15.9 Hz), 7.08 (1H, d, *J* = 2.0 Hz), 7.02 (1H, dd, *J* = 8.2 Hz), 6.87 (1H, d, *J* = 8.2 Hz), 6.27 (1H, d, *J* = 15.9 Hz), 3.8 (3H, s).

Preparation of phosphate buffer solutions

Phosphate buffer solutions were prepared from KH_2PO_4 and K_2HPO_4 salts, dissolved in water (H_2O or D_2O) and titrated with strong acid (HCl or DCl), or base (NaOH or NaOD) until desired pH (pD) was reached. pD was adjusted considering the correction for measuring with glass electrode in D_2O, pD = pH + 0.41 (37). pH was measured with pH meter Mettler Toledo MP 230 equipped with combined pH electrode Mettler Toledo, InLab Semi-Micro with precision of ± 0.01. The concentration of phosphate buffer solution for kinetic measurements was 0.02 mol L^{-1} for pH (pD) 5.9 and 0.1 mol L^{-1} for pH (pD) 7.2, and for determination of Fe(II) methyl caffeate complex 0.01 mol L^{-1}. The solutions were prepared weekly and stored at 4 °C.

Kinetic measurements

Pseudo-first-order rate constants for the reactions of the MC and CA with the DPPH• radical were determined spectrophotometrically by monitoring the decrease in DPPH• absorbance at 518 nm. All spectral and absorbance-time data were collected using an Avantes AvaSpec 2048L StarLine spectrometer (Avantes B.V., The Netherlands), equipped with a Quantum Northwest QPOD temperature-controlled sample compartment for fiber optic spectroscopy. For the pseudo-first-order rate constants greater than 0.1 s^{-1} ($t_{1/2} < 7$ s) the stopped-flow instrument RX2000 Rapid kinetics (Applied Photophysics, UK) for rapid mixing of reactants was used. Kinetic measurements were conducted under strictly controlled temperature conditions, maintained within ± 0.1 °C. The stability of DPPH• was evaluated under all experimental conditions used in the study (reaction media without antioxidants MC or CA), and no changes in its concentration were observed.

Stock solutions of the reactants were freshly prepared each day by dissolving MC, CA or DPPH• in 1,4-dioxane. Prior to initiating the reaction, the reaction medium was

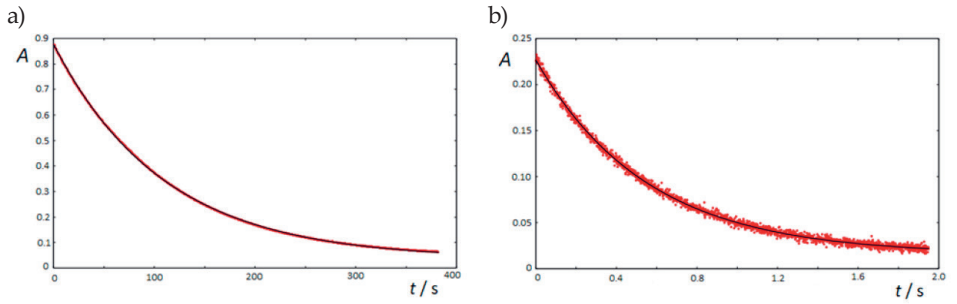

Fig. 2. Kinetic traces at 518 nm for the reaction of methyl caffeate and DPPH• at 25.0 °C. a) 1,4-dioxane: phosphate buffer pH 5.9 (0.95:0.05, *V*/*V*), c(MC) = 0.005 mol L^{-1}, c(DPPH•) = 0.00008 mol L^{-1}, k_{obs} = 0.00916 s^{-1}; b) 1,4-dioxane:phosphate buffer pH 7.2 (0.85:0.15, *V*/*V*), c(MC) = 0.0005 mol L^{-1}, c(DPPH•) = 0.000025 mol L^{-1}, k_{obs} = 1.82 s^{-1}.

thermostated for 20 minutes. The reaction was started by adding an appropriate volume of the DPPH• stock solution to the thermostated reaction medium. For stopped-flow kinetic experiments, reactant solutions were prepared at twice the desired final concentrations and mixed in a 1:1 volumetric ratio. In a typical kinetic run, at least 200 absorbance-time data points were collected and analysed using a standard least-squares fitting algorithm. To determine the rate parameters under the specified conditions, a minimum of three to four pseudo-first-order rate constants were used. All measurements were conducted under pseudo-first-order conditions, with MC or CA concentrations maintained at least 10-fold in excess, with the exception of the fastest kinetics in alkaline media, in which the ratio of CA to DPPH• was from 5–17.5. Very good pseudo-first-order kinetic behaviour was consistently observed (Fig. 2).

Calculation of second-order rate constants, KIEs and thermodynamic activation parameters

Second-order reaction rate constants, k_2, were determined from the slopes of plots of the observed pseudo-first-order rate constants k_{obs} *vs.* the concentration of MC or CA (Fig. 3a). In accordance with previously determined stoichiometry ArOH:DPPH• = 1:2 for the reaction of several other phenols with DPPH• (35, 38), the rate law for the reaction of MC or CA and DPPH• can be written as:

$$-\frac{\mathrm{d}[\mathrm{DPPH}\bullet]}{\mathrm{d}t} = 2k_2[\mathrm{DPPH}\bullet][\mathrm{ArOH}] \tag{4}$$

$$k_{obs} = 2\,k_2\,[\mathrm{ArOH}] \tag{5}$$

In all the reaction conditions applied in this study, the dependence of k_{obs} *vs.* [MC] or [CA] was strongly linear.

KIEs were determined following the equation:

$$\mathrm{KIE} = k_{2,\mathrm{ArOH}} / k_{2,\mathrm{ArOD}} \tag{6}$$

ArOD was obtained by dissolving MC or CA in 1,4-dioxane-D_2O solvent mixture, due to the rapid exchange of phenol OH hydrogens with deuterium.

Thermodynamic activation parameters were calculated from second-order rate constants measured over the temperature range of 14–45 °C, using well-known Arrhenius and Eyring equations:

$$\ln k_2 = \ln A - \frac{E_a}{RT} \tag{7}$$

$$\ln \frac{k_2}{T} = -\frac{\Delta H^{\ddagger}}{R}\frac{1}{T} + \ln \frac{k_B}{h} + \frac{\Delta S^{\ddagger}}{R} \tag{8}$$

Computational methods

The DFT calculations were carried out using the GAUSSIAN 16 software (39) at the (U)B3LYP/def2-TZVPP level of theory with the non-specific solvent effects estimated by using the polarisable continuum model (PCM) of the self-consistent reaction field (SCRF) method (40) with 1,4-dioxane as a solvent. The stationary points obtained by geometry optimisations were confirmed either as minima or saddle points by vibrational analysis at the same theory level. The obtained transition state structure was explored with intrinsic reaction coordinate (IRC) analysis (41) at the same theory level and the intrinsic bond orbital (IBO) localisation procedure (42–44) with the IBOVIEW program (45). Estimation of the tunnelling correction for the calculated reaction constants and KIE was done using the Wigner method with the TAMkin program (46).

Spectrophotometric determination of Fe(II) methyl caffeate complex

The formation of a complex between Fe(II) and MC was determined spectrophotometrically. UV-VIS absorption spectra were measured using an HP 8453 spectrophotometer. Complex formation was studied in 0.01 mol L^{-1} phosphate buffer. The buffer solution was bubbled with nitrogen for 1 hour prior to measurement. Aqueous solution of MC (0.003 mol L^{-1}) and $FeSO_4$ (0.02 mol L^{-1}) were freshly prepared before measurement. Complex formation was initiated by adding the Fe(II) solution to the MC solution in the buffer.

RESULTS AND DISCUSSION

Experimental evidence of hydrogen transfer in reaction of methyl caffeate and DPPH•

In recent decades, numerous studies have examined the reactivity of MC and other alkyl caffeates toward DPPH•, consistently reporting significant scavenging activity – often surpassing that of some traditional antioxidants, based on IC_{50} values (5, 9, 10, 20, 29). In contrast, only one experimental study has explored the kinetics and mechanism of the reaction between MC and DPPH• in polar solvents (methanol and ethanol), identifying SPLET (fast ET from the catecholate anion) as the predominant mechanism (33, 35). Nevertheless, *in silico* studies of the reactions of phenolic antioxidants with free radicals point to the possible HAT/PCET mechanism in the case of nonpolar reaction medium (22, 33, 38, 47).

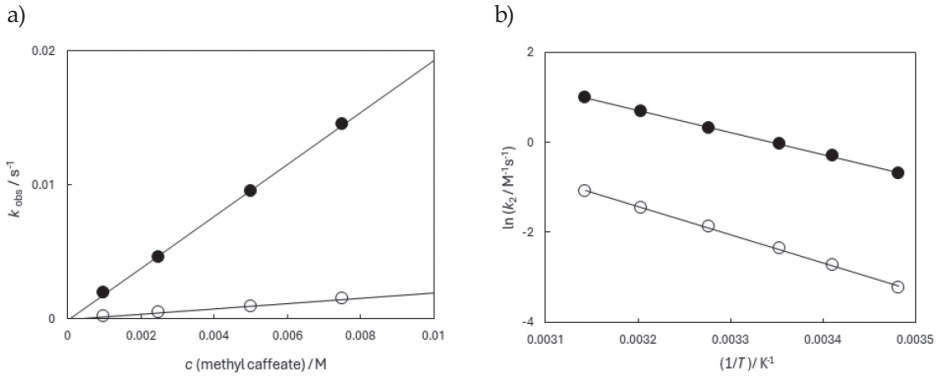

Fig. 3. a) The plot of pseudo-first order constants (k_{obs}) *vs.* concentration of methyl caffeate for the reaction of methyl caffeate and DPPH• in 1,4-dioxane:phosphate buffer pH 5.9 (0.95:0.05, *V*/*V*) (●) and 1,4-dioxane:phosphate buffer pD 5.9 (0.95:0.05, *V*/*V*) (○) at 25 °C, *c*(DPPH•) = 0.00008 mol L^{-1}; b) Arrhenius plots of ln $k_{2,H}$ (●) or ln $k_{2,D}$ (○) *vs.* 1/*T* for the reaction of methyl caffeate and DPPH• in 1,4-dioxane:phosphate buffer pH(D) 5.9 (0.95:0.05, *V*/*V*).

In this study, we investigated the kinetic behaviour of MC toward DPPH• to determine the rate constant and elucidate the reaction mechanism in a predominantly nonpolar medium. The reaction medium consisted of 1,4-dioxane and phosphate buffer at pH 5.9 or 7.2, in two different solvent volume ratios: 0.95:0.05 or 0.85:0.15 (*V*/*V*). The buffered medium was used to eliminate potential traces of acidic or basic impurities that could affect the concentration of different forms of the reactant MC (neutral or anionic), or cause deviations from the linear dependence of the observed rate constants, k_{obs}, on concentration of MC (Fig. 3a).

Table I. Second-order rate constants k_2 *and kinetic isotope effects (KIE) for the reaction of methyl caffeate or caffeic acid and DPPH• in different reaction media, at 25 °C; values reported as mean (SD)*

Reaction medium	Methyl caffeate		Caffeic acid	
	k_2/mol^{-1} L s^{-1}	KIE	k_2/mol^{-1} L s^{-1}	KIE
1,4-dioxane:phosphate buffer pH(D) 5.9 (0.95:0.05, *V*/*V*)[a]	0.965 (0.014)	9.93 (0.39)	1.103 (0.007)	9.18 (0.12)
1,4-dioxane:phosphate buffer pH(D) 5.9 (0.85:0.15, *V*/*V*)[b]	12.5 (0.3)	1.66 (0.08)		
1,4-dioxane:phosphate buffer pH 7.2 (0.85:0.15, *V*/*V*)[c]	1443 (72)		639 (8)	
1,4-dioxane:water (0.95:0.05, *V*/*V*), 3 × 10^{-4} mol L^{-1} NaOH or NaOD[d]			4147 (230)	1.02 (0.18)

[a] 0.001–0.0075 mol L^{-1} MC or CA, 0.00008 mol L^{-1} DPPH•; [b] 0.0005–0.003 mol L^{-1} MC, 0.00005 mol L^{-1} DPPH•; [c] 0.00025–0.001 mol L^{-1} MC or CA, 0.000025 mol L^{-1} DPPH•; [d] 0.00005–0.000175 mol L^{-1} CA, 0.00001 mol L^{-1} DPPH•.

At pH 5.9, MC is expected to be in its neutral form (catechol OH groups fully protonated), based on the assumption that the pK_a value of the catechol OH group in MC is even greater than 8.35, the value determined in water (48). The value of the second-order rate constants, k_2, determined in the 0.95:0.05 (*V*/*V*) mixture of 1,4-dioxane and phosphate buffer at pH 5.9, were nearly identical for MC and CA in reaction with DPPH•, with values of 0.965 and 1.103 mol^{-1} L s^{-1}, respectively (Table I).

When the volume fraction of the polar solvent (phosphate buffer, pH 5.9) was increased to 0.85:0.15 (*V*/*V*), the rate constant for MC increased by an order of magnitude to 12.5 mol^{-1} L s^{-1}, indicating the presence of the anionic form of MC. Even small amounts of the catecholate anion can significantly enhance the rate constant and are connected to SPLET reaction mechanism, as previously observed in the study by Foti *et al*. (35). This effect became even more pronounced when the buffer pH was raised to 7.2, resulting in a further two-order-of-magnitude increase in the rate constant, reaching a value of 1443 mol^{-1} L s^{-1}. Furthermore, in reaction of CA and DPPH• in 0.95:0.05 (*V*/*V*) mixture of 1,4-dioxane and water in presence of alkali (pH > 10) where the dominant form catecholate anion is expected, the rate constant reached the value of 4147 mol^{-1} L s^{-1}.

The kinetic isotope effect (KIE), an important parameter for determining whether proton transfer is involved in the rate-determining step of a reaction, was calculated using experiments conducted in solvent mixtures containing phosphate buffer prepared in D_2O at pD 5.9. The primary KIE is defined as the ratio of reaction rate constants for processes involving the formation or cleavage of a bond with the lighter isotope (hydrogen, H) compared to the same reaction involving the heavier isotope (deuterium, D) (Equation *6*). For OH bonds, the upper limit of the kinetic isotope effect (KIE) within the framework of semi-classical theory is 8. This value can increase to a maximum of 13 when bending vibrations are included in the calculation (49). In our study, the KIE for the reaction between MC and DPPH• in a 0.95:0.05 (*V*/*V*) mixture of 1,4-dioxane and phosphate buffer at pH(D) 5.9 was 9.93 (Table I). The observed KIE value eliminates SPLET as a possible reaction mechanism in these experimental conditions. However, when the solvent ratio was changed to 0.85:0.15 (*V*/*V*), the KIE significantly decreased to 1.66. This pronounced difference may serve as experimental evidence for a mechanistic shift – from a slower HAT/PCET mechanism to a much faster SPLET mechanism – due to the presence of small amounts of the catecholate anion.

Thermodynamic activation parameters for the reaction between MC and DPPH• in a 0.95:0.05 (*V*/*V*) mixture of 1,4-dioxane and phosphate buffer at pH 5.9 were determined through kinetic measurements over the temperature range of 14–45 °C (Fig. 3b, Table II). The values obtained closely match those reported for the reaction of CA with DPPH• in a 0.95:0.05 (*V*/*V*) mixture of 1,4-dioxane and water, as described in a previous study (38). The ratio of Arrhenius pre-exponential factors, A_H/A_D, which deviates from the semi-classical limits of 0.7–1.2, along with isotopic difference in activation energy (ΔE_a) exceeding 5.1 kJ mol^{-1} for OH bond dissociation, are characteristic indicators of hydrogen tunnelling in the reaction (49, 50). For the MC and DPPH• reaction, these values were 0.11 for A_H/A_D and 11.2 kJ mol^{-1} for ΔE_a, both outside the range predicted by semi-classical models, similar as those in the CA-DPPH• system (38). Combined with the observed KIE, these findings strongly support the presence of hydrogen tunnelling in this reaction and are consistent with observations from reactions involving structurally similar antioxidants – CA, hydroxytyrosol, and homovanillyl alcohol (38) – as well as the reaction of α-tocopherol

with DPPH• (51). Furthermore, hydrogen tunnelling has been experimentally confirmed in other antioxidant reactions, such as those involving vitamin C with TEMPO• (52) and hexacyanoferrate(III) ions (53).

Table II. Thermodynamic activation parameters for the reaction of methyl caffeate and DPPH• in 0.95:0.05, V/V 1,4-dioxane:phosphate buffer pH(D) 5.9 solvent mixture at 25 °C[a]

Reaction medium	$\Delta G^{\ddagger}$ / kJ mol^{-1}	$\Delta H^{\ddagger}$ / kJ mol^{-1}	$\Delta S^{\ddagger}$ / J K^{-1} mol^{-1}	E_a / kJ mol^{-1}	ln (A/mol^{-1} L s^{-1})
1,4-dioxane:phosphate buffer pH 5.9	73.2 (0.7)	38.3 (0.5)	–117.1 (1.7)	40.8 (0.5)	16.4 (0.2)
1,4-dioxane:phosphate buffer pD 5.9	79.0 (1.4)	49.5 (1.0)	–98.7 (3.2)	52.0 (0.9)	18.6 (0.4)

[a] Values reported as mean (SD).

Altogether, the experimental evidence points to the concerted HAT/PCET mechanism in the reaction of between MC and DPPH• in predominantly nonpolar medium, but to differentiate these two mechanisms, the calculation methods must be employed.

Computational analysis of hydrogen transfer in the reaction of methyl caffeate and DPPH•

For the proposed hydrogen transfer from MC to DPPH•, a transition structure (TS) calculation was performed, as well as an intrinsic reaction coordinate (IRC) (41) and intrinsic bond orbital (IBO) analysis (42–44). The obtained TS structure involves a reaction at the 3′-OH moiety, the MC reaction site that was found to be the most reactive by bond dissociation enthalpy (BDE) analysis (24). The hydrogen-donor (H···O) and hydrogen-acceptor (N···H) distances for the TS are 1.265 Å and 1.216 Å, respectively, and the N···H···O angle is 176.6°. These values are comparable to the corresponding distances and angles obtained for calculated TS in hydrogen atom transfer reactions to DPPH• from phenol, *p*-metoxyphenol (23), homovanillyl alcohol, hydroxytyrosol and CA (38). The calculated Gibbs activation energy of 83.8 kJ mol^{-1} agrees with the experimental value, in support of the proposed TS structure obtained. The calculated KIE_{TUNN} (with tunnelling correction) is 20.2. IBO analysis proposed by Knizia (43) enables the visualisation of molecular orbitals and electronic structure changes along reaction paths (42–44). IBO analysis has proven to be useful in researching and interpreting reaction mechanisms. In hydrogen transfer reactions, it has been shown that IBO analysis can unambiguously distinguish between HAT and PCET processes (44). Representative IBOs involved in hydrogen transfer from MC to DPPH• plotted along the IRC obtained from DFT calculations are shown in Fig. 4. As can be seen, the β electron (A, blue IBO) transferred to the DPPH• N atom that has an unpaired α electron (not shown) comes from the aromatic ring orbital of the MC, leaving an unpaired α electron (A, green IBO) on it as well. The proton from the MC's OH group is transferred separately from the electron to the IBOs (B, green and blue IBOs) located on the second N atom of DPPH•. The obtained results from DFT calculations clearly point to a PCET reac-

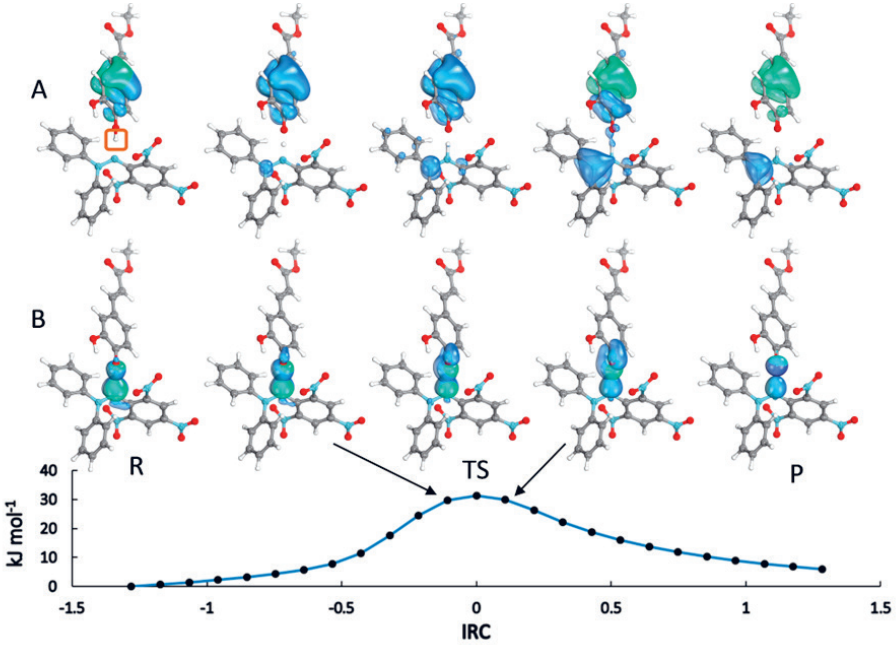

Fig. 4. Changes in α (green) and β (blue) intrinsic bond orbitals (IBOs) involved in electron transfer (A) and proton transfer (B), energy plotted along the intrinsic reaction coordinate (IRC) path for hydrogen transfer from methyl caffeate (MC) to DPPH• obtained from the DFT calculations. R – activated complex resembling the reactants, TS – transition structure, P – activated complex resembling the products. Normal mode displacement vector for a unique imaginary frequency of 1705.4 i cm^{-1} is associated with a motion of the H atom (marked) of the O-H moiety of MC to the N atom of DPPH•.

tion mechanism, since proton transfer and electron transfer are separate and from different reaction sites and also involve different orbitals.

Formation of Fe(II) methyl caffeate complex

The formation of a complex between Fe(II) and MC was monitored spectrophotometrically in aqueous phosphate buffer at pH 7.0. Upon the addition of Fe(II) to the MC solution, the absorbance maxima shifted from 297 and 323 nm, corresponding to MC spectrum, to 355 nm and new absorbance peaks appeared with maxima at 512 and 600 nm (Figs. 5 and 6). The spectral changes are attributed to the formation of the Fe(II) MC complex, in which iron is coordinated by the catechol moiety. Complex formation is pH-dependent, with decreased stability in acidic solution (Fig. 7). Measurements were conducted under nitrogen to prevent oxidation of Fe(II) to Fe(III) (54). Under the same conditions (aqueous phosphate buffer at pH 7.0), the spectrum of the Fe(II) caffeate complex was measured, showing a maximum absorption at 600 nm.

Sørensen *et al.* previously reported the formation of Fe(II) MC complex in sodium acetate-imidazole buffer at pH 7 (29). The formation of these complexes was influenced by

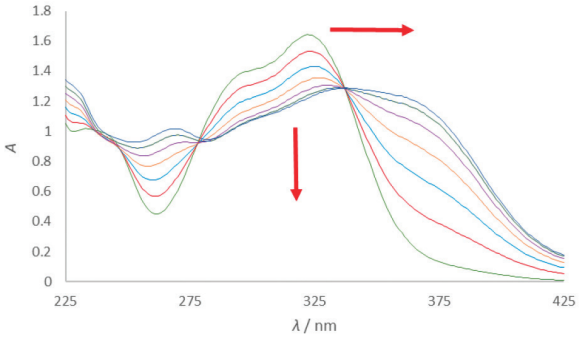

Fig. 5. UV absorption spectra of Fe(II) methyl caffeate complex in the mixture of methyl caffeate (10^{-4} mol L^{-1}) and various concentrations of Fe(II) (10^{-5} to 10^{-4} mol L^{-1}) in aqueous phosphate buffer at pH = 7.0 (spectra of phosphate buffer are subtracted).

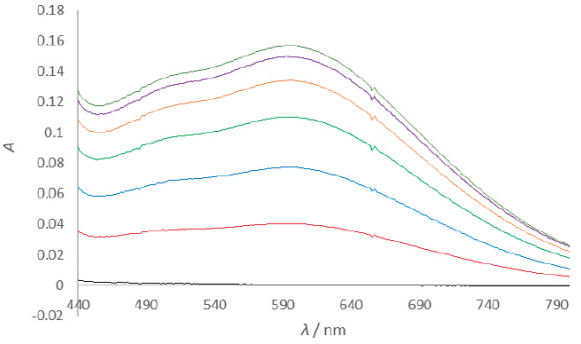

Fig. 6. VIS absorption spectra of Fe(II) methyl caffeate complex in the mixture of methyl caffeate (10^{-4} mol L^{-1}) and various concentrations of Fe(II) (10^{-5} to 10^{-4} mol L^{-1}) in aqueous phosphate buffer at pH = 7.0 (spectra of phosphate buffer are subtracted).

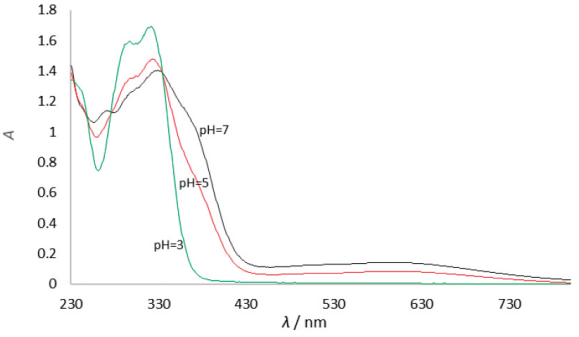

Fig. 7. pH-dependence of Fe(II) methyl caffeate complex formation in the mixture of methyl caffeate (10^{-4} mol L^{-1}) and Fe(II) (10^{-4} mol L^{-1}) in aqueous phosphate buffer (spectra of phosphate buffer are subtracted).

the medium and buffer composition (29, 30). Since complex formation occurs at pH 7, it has physiological significance. The formation of Fe(II) complexes with caffeate and caffeic acid esters, including phenylethyl caffeate, benzyl caffeate, and 3-methyl-2-butenyl caffeate, has also been determined previously (30, 55–57). Phenylethyl caffeate has shown stronger iron-binding ability than caffeic acid (56). Fe(II) complexed with MC is expected to be less active toward H_2O_2 than free Fe(II), thereby reducing hydroxyl radical generation under physiological conditions.

CONCLUSIONS

This study provides compelling experimental and computational evidence that MC acts as a potent antioxidant *via* a PCET mechanism, with hydrogen tunnelling contributing to its reactivity in nonpolar media. The kinetic and thermodynamic parameters, supported by DFT and IBO analyses, confirm the mechanistic pathway. Furthermore, the ability of MC to form stable Fe(II) complexes at physiological pH, while reducing hydroxyl radical formation, highlights its potential as a metal-chelating antioxidant. These insights enhance our understanding of the antioxidant properties of MC and support its further development in therapeutic and industrial applications.

Acknowledgements. – The authors would like to thank Prof. Monika Barbarić (University of Zagreb Faculty of Pharmacy and Biochemistry, Croatia) for her assistance with the synthesis of methyl caffeate.

Conflicts of interest. – The authors declare no conflict of interest.

Funding. – This research was funded by strengthening the scientific research and innovation capacities of the Faculty of Pharmacy and Biochemistry, University of Zagreb (FarmInova; project number KK.01.1.1.02.0021), financed by the European Regional Development Fund, Operational Program Competitiveness and Cohesion for the period 2014–2020, and supported by the University of Zagreb (support for 2022).

Authors contributions. – Conceptualisation, A.K.M.; methodology, A.K.M., V.P., and C.J.B.; formal analysis A.K.M., V.P., C.J.B., A.R., and A.Š.; investigation, A.K.M., V.P., C.J.B., A.R., and A.Š.; writing – original draft preparation, A.K.M., V.P., and C.J.B.; writing – review and editing, A.K.M.; visualization, A.K.M., V.P., and C.J.B.; supervision, A.K.M.; funding acquisition, A.K.M., V.P., and C.J.B.

REFERENCES

1. A. P. Gomes Da Silva, W. G. Sganzerla, O. D. John and R. Marchiosi, A comprehensive review of the classification, sources, biosynthesis, and biological properties of hydroxybenzoic and hydroxycinnamic acids, *Phytochem. Rev.* **24**(2) (2025) 1061–1090; https://doi.org/10.1007/s11101-023-09891-y
2. M. Martiniakova, A. Sarocka, N. Penzes, R. Biro, V. Kovacova, V. Mondockova, A. Sevcikova, S. Ciernikova and R. Omelka, Protective role of dietary polyphenols in the management and treatment of type 2 diabetes mellitus, *Nutrients* **17**(2) (2025) Article ID 275 (41 pages); https://doi.org/10.3390/nu17020275
3. M. K. Mandal and A. J. Domb, Antimicrobial activities of natural bioactive polyphenols, *Pharmaceutics* **16**(6) (2024) Article ID 718 (25 pages); https://doi.org/10.3390/pharmaceutics16060718
4. F. Khan, N. I. Bamunuarachchi, N. Tabassum and Y.-M. Kim, Caffeic acid and its derivatives: Antimicrobial drugs toward microbial pathogens, *J. Agric. Food Chem.* **69**(10) (2021) 2979–3004; https://doi.org/10.1021/acs.jafc.0c07579

5. J. Wang, S.-S. Gu, N. Pang, F.-Q. Wang, F. Pang, H.-S. Cui, X.-Y. Wu and F.-A. Wu, Alkyl caffeates improve the antioxidant activity, antitumor property and oxidation stability of edible oil, *PLoS ONE* **9**(4) (2014) e95909 (10 pages); https://doi.org/10.1371/journal.pone.0095909
6. Y. Wang, M. Zheng, Q. Jiang, Y. Xu, X. Zhou, N. Zhang, D. Sun, H. Li and L. Chen, Chemical components of the fruits of *Morus nigra* Linn.: Methyl caffeate as a potential anticancer agent by targeting 3-phosphoglycerate dehydrogenase, *J. Agric. Food Chem.* **69**(42) (2021) 12433–12444; https://doi.org/10.1021/acs.jafc.1c03215
7. D. Lee, Y. Qi, R. Kim, J. Song, H. Kim, H. Y. Kim, D. S. Jang and K. S. Kang, Methyl caffeate isolated from the flowers of *Prunus persica* (L.) Batsch enhances glucose-stimulated insulin secretion, *Biomolecules* **11**(2) (2021) Article ID 279 (13 pages); https://doi.org/10.3390/biom11020279
8. A. Balachandran, N. Emi, Y. Arun, Y. Yamamoto, B. Ahilan, B. Sangeetha, V. Duraipandiyan, Y. Inaguma, A. Okamoto, S. Ignacimuthu, N. A. Al-Dhabi and P. T. Perumal, In vitro anticancer activity of methyl caffeate isolated from *Solanum torvum* Swartz. fruit, *Chem.-Biol. Interact.* **242** (2015) 81–90; https://doi.org/10.1016/j.cbi.2015.09.023
9. Q. Q. Chen, H. Pasdar and X. C. Weng, Butylated methyl caffeate: A novel antioxidant, *Grasas aceites* **71**(2) (2020) e352 (8 pages); https://doi.org/10.3989/gya.0226191
10. N. Masuoka and I. Kubo, Suppression of superoxide anion generation catalyzed by xanthine oxidase with alkyl caffeates and the scavenging activity, *Int. J. Food Sci. Nutr.* **67**(3) (2016) 283–287; https://doi.org/10.3109/09637486.2016.1153609
11. T. Masuda, K. Yamada, J. Akiyama, T. Someya, Y. Odaka, Y. Takeda, M. Tori, K. Nakashima, T. Maekawa and Y. Sone, Antioxidation mechanism studies of caffeic acid: Identification of antioxidation products of methyl caffeate from lipid oxidation, *J. Agric. Food Chem.* **56**(14) (2008) 5947–5952; https://doi.org/10.1021/jf800781b
12. H. M. Eid, F. Thong, A. Nachar and P. S. Haddad, Caffeic acid methyl and ethyl esters exert potential antidiabetic effects on glucose and lipid metabolism in cultured murine insulin-sensitive cells through mechanisms implicating activation of AMPK, *Pharm. Biol.* **55**(1) (2017) 2026–2034; https://doi.org/10.1080/13880209.2017.1345952
13. G. R. Gandhi, S. Ignacimuthu, M. G. Paulraj and P. Sasikumar, Antihyperglycemic activity and antidiabetic effect of methyl caffeate isolated from *Solanum torvum* Swartz. fruit in streptozotocin induced diabetic rats, *Eur. J. Pharmacol.* **670**(2–3) (2011) 623–631; https://doi.org/10.1016/j.ejphar.2011.09.159
14. N. Putra, G. Faroliu, N. Syafni, Nofrizal, A. Bakhtiar and D. Arbain, Isolation and antibacterial properties of phenyl acrylic acid derivatives from *Balanophora elongata* Blume, *J. Math. Fund. Sci.* **53**(2) (2021) 231–242; https://doi.org/10.5614/j.math.fund.sci.2021.53.2.5
15. A. Balachandran, V. Duraipandiyan, N. A. Al-Dhabi, K. Balakrishna, N. P. Kalia, V. S. Rajput, I. A. Khan and S. Ignacimuthu, Antimicrobial and antimycobacterial activities of methyl caffeate isolated from *Solanum torvum* Swartz. Fruit, *Indian J. Microbiol.* **52**(4) (2012) 676–681; https://doi.org/10.1007/s12088-012-0313-8
16. H. Lim, B. K. Park, S. Y. Shin, Y. S. Kwon and H. P. Kim, Methyl caffeate and some plant constituents inhibit age-related inflammation: Effects on senescence-associated secretory phenotype (SASP) formation, *Arch. Pharm. Res.* **40**(4) (2017) 524–535; https://doi.org/10.1007/s12272-017-0909-y
17. K.-M. Shin, I.-T. Kim, Y.-M. Park, J. Ha, J.-W. Choi, H.-J. Park, Y. S. Lee and K.-T. Lee, Anti-inflammatory effect of caffeic acid methyl ester and its mode of action through the inhibition of prostaglandin E2, nitric oxide and tumor necrosis factor-α production, *Biochem. Pharmacol.* **68**(12) (2004) 2327–2336; https://doi.org/10.1016/j.bcp.2004.08.002
18. A. Jantas, J. Chwastek, J. Malarz, A. Stojakowska and W. Lasoń, Neuroprotective effects of methyl caffeate against hydrogen peroxide-induced cell damage: Involvement of caspase 3 and cathepsin d inhibition, *Biomolecules* **10**(11) (2020) Article ID 1530 (22 pages); https://doi.org/10.3390/biom10111530

19. J.-Z. Wang, C.-H. Yan, X.-R. Zhang, Q.-B. Tu, Y. Xu, S. Sheng, F.-A. Wu and J. Wang, A novel nanoparticle loaded with methyl caffeate and caffeic acid phenethyl ester against *Ralstonia solanacearum* – a plant pathogenic bacteria, *RSC Adv.* **10**(7) (2020) 3978–3990; https://doi.org/10.1039/C9RA09441E
20. J. Garrido, A. Gaspar, E. M. Garrido, R. Miri, M. Tavakkoli, S. Pourali, L. Saso, F. Borges and O. Firuzi, Alkyl esters of hydroxycinnamic acids with improved antioxidant activity and lipophilicity protect PC12 cells against oxidative stress, *Biochimie* **94**(4) (2012) 961–967; https://doi.org/10.1016/j.biochi.2011.12.015
21. R. Amorati and L. Valgimigli, Modulation of the antioxidant activity of phenols by non-covalent interactions, *Org. Biomol. Chem.* **10**(21) (2012) Article ID 4147 (12 pages); https://doi.org/10.1039/c2ob25174d
22. K. U. Ingold and D. A. Pratt, Advances in radical-trapping antioxidant chemistry in the 21st century: A kinetics and mechanisms perspective, *Chem. Rev.* **114**(18) (2014) 9022–9046; https://doi.org/10.1021/cr500226n
23. M. C. Foti, C. Daquino, I. D. Mackie, G. A. DiLabio and K. U. Ingold, Reaction of Phenols with the 2,2-diphenyl-1-picrylhydrazyl radical. Kinetics and DFT calculations applied to determine ArO-H bond dissociation enthalpies and reaction mechanism, *J. Org. Chem.* **73**(23) (2008) 9270–9282; https://doi.org/10.1021/jo8016555
24. A. Urbaniak, J. Kujawski, K. Czaja and M. Szelag, Antioxidant properties of several caffeic acid derivatives: A theoretical study, *C. R. Chim.* **20**(11-12) (2017) 1072–1082; https://doi.org/10.1016/j.crci.2017.08.003
25. R. Tyburski, T. Liu, S. D. Glover and L. Hammarström, Proton-coupled electron transfer guidelines, fair and square, *J. Am. Chem. Soc.* **143**(2) (2021) 560–576; https://doi.org/10.1021/jacs.0c09106
26. C. G. Pierpont and C. W. Lange, *The Chemistry of Transition Metal Complexes Containing Catechol and Semiquinone Ligands*, in *Progress in Inorganic Chemistry*, (Ed. K. D. Karlin), Vol. 41, Wiley, New York 1994, 331–442; https://doi.org/10.1002/9780470166420.ch5
27. S. Borowska, M. M. Brzoska and M. Tomczyk, Complexation of bioelements and toxic metals by polyphenolic compounds – implications for health, *Curr. Drug Targets* **19**(14) (2018) 1612–1638; https://doi.org/10.2174/1389450119666180403101555
28. D. Galaris, A. Barbouti and K. Pantopoulos, Iron homeostasis and oxidative stress: An intimate relationship, *Biochim. Biophys. Acta Mol. Cell Res.* **1866**(12) (2019) Article ID 118535 (15 pages); https://doi.org/10.1016/j.bbamcr.2019.118535
29. A.-D. M. Sørensen, E. Durand, M. Laguerre, C. Bayrasy, J. Lecomte, P. Villeneuve and C. Jacobsen, Antioxidant properties and efficacies of synthesized alkyl caffeates, ferulates, and coumarates, *J. Agric. Food Chem.* **62**(52) (2014) 12553–12562; https://doi.org/10.1021/jf500588s
30. M. Andjelkovic, J. Vancamp, B. Demeulenaer, G. Depaemelaere, C. Socaciu, M. Verloo and R. Verhe, Iron-chelation properties of phenolic acids bearing catechol and galloyl groups, *Food Chem.* **98**(1) (2006) 23–31; https://doi.org/10.1016/j.foodchem.2005.05.044
31. S. Khokhar and R. K. Owusu Apenten, Iron binding characteristics of phenolic compounds: Some tentative structure-activity relations, *Food Chem.* **81**(1) (2003) 133–140; https://doi.org/10.1016/S0308-8146(02)00394-1
32. G. Mazzone, On the inhibition of hydroxyl radical formation by hydroxycinnamic acids: The case of caffeic acid as a promising chelating ligand of a ferrous ion, *J. Phys. Chem. A* **123**(44) (2019) 9560–9566; https://doi.org/10.1021/acs.jpca.9b08384
33. M. C. Foti, Use and abuse of the DPPH$^{\bullet}$ radical, *J. Agric. Food Chem.* **63**(40) (2015) 8765–8776; https://doi.org/10.1021/acs.jafc.5b03839
34. P. Przybylski, A. Konopko, P. Łętowski, K. Jodko-Piórecka and G. Litwinienko, Concentration--dependent HAT/ET mechanism of the reaction of phenols with 2,2-diphenyl-1-picrylhydrazyl (DPPH$^{\cdot}$) in methanol, *RSC Adv.* **12**(13) (2022) 8131–8136; https://doi.org/10.1039/d2ra01033j

35. M. C. Foti, C. Daquino and C. Geraci, Electron-transfer reaction of cinnamic acids and their methyl esters with the DPPH • radical in alcoholic solutions, *J. Org. Chem.* **69**(7) (2004) 2309–2314; https://doi.org/10.1021/jo035758q
36. J. Wang, S. Gu, N. Pang, F. Wang and F. Wu, A study of esterification of caffeic acid with methanol using *p*-toluenesulfonic acid as a catalyst, *J. Serb. Chem. Soc.* **78**(7) (2013) 1023–1034; https://doi.org/10.2298/JSC120802101W
37. A. K. Covington, M. Paabo, R. A. Robinson and R. G. Bates, Use of the glass electrode in deuterium oxide and the relation between the standardized pD (pa_D) scale and the operational pH in heavy water, *Anal. Chem.* **40**(4) (1968) 700–706; https://doi.org/10.1021/ac60260a013
38. J. Torić, A. Karković Marković, S. Mustać, A. Pulitika, C. Jakobušić Brala and V. Pilepić, Proton-coupled electron transfer and hydrogen tunneling in olive oil phenol reactions, *Int. J. Mol. Sci.* **25**(12) (2024) Article ID 6341 (15 pages); https://doi.org/10.3390/ijms25126341
39. Gaussian 16, Revision C.02, M. J. Frisch, G. W. Trucks, H. B. Schlegel, G. E. Scuseria, M. A. Robb, J. R. Cheeseman, G. Scalmani, V. Barone, G. A. Petersson, H. Nakatsuji, X. Li, M. Caricato, A. V. Marenich, J. Bloino, B. G. Janesko, R. Gomperts, B. Mennucci, H. P. Hratchian, J. V. Ortiz, A. F. Izmaylov, J. L. Sonnenberg, D. Williams-Young, F. Ding, F. Lipparini, F. Egidi, J. Goings, B. Peng, A. Petrone, T. Henderson, D. Ranasinghe, V. G. Zakrzewski, J. Gao, N. Rega, G. Zheng, W. Liang, M. Hada, M. Ehara, K. Toyota, R. Fukuda, J. Hasegawa, M. Ishida, T. Nakajima, Y. Honda, O. Kitao, H. Nakai, T. Vreven, K. Throssell, J. A. Montgomery, Jr., J. E. Peralta, F. Ogliaro, M. J. Bearpark, J. J. Heyd, E. N. Brothers, K. N. Kudin, V. N. Staroverov, T. A. Keith, R. Kobayashi, J. Normand, K. Raghavachari, A. P. Rendell, J. C. Burant, S. S. Iyengar, J. Tomasi, M. Cossi, J. M. Millam, M. Klene, C. Adamo, R. Cammi, J. W. Ochterski, R. L. Martin, K. Morokuma, O. Farkas, J. B. Foresman and D. J. Fox, Gaussian, Inc., Wallingford CT, 2016.
40. J. Tomasi, B. Mennucci and R. Cammi, Quantum mechanical continuum solvation models, *Chem. Rev.* **105**(8) (2005) 2999–3094; https://doi.org/10.1021/cr9904009
41. K. Fukui, The path of chemical reactions – the IRC approach, *Acc. Chem. Res.* **14**(12) (1981) 363–368; https://doi.org/10.1021/ar00072a001
42. G. Knizia and J. E. M. N. Klein, Electron flow in reaction mechanisms – revealed from first principles, *Ang. Chem. Int. Ed.* **54**(18) (2015) 5518–5522; https://doi.org/10.1002/anie.201410637
43. G. Knizia, Intrinsic atomic orbitals: An unbiased bridge between quantum theory and chemical concepts, *J. Chem. Theory Comput.* **9**(11) (2013) 4834–4843; https://doi.org/10.1021/ct400687b
44. J. E. M. N. Klein and G. Knizia, cPCET versus HAT: A direct theoretical method for distinguishing X–H bond-activation mechanisms, *Ang. Chem. Int. Ed.* **57**(37) (2018) 11913–11917; https://doi.org/10.1002/anie.201805511
45. G. Knizia, IboView, http://www.iboview.org.
46. A. Ghysels, T. Verstraelen, K. Hemelsoet, M. Waroquier and V. Van Speybroeck, TAMkin: A versatile package for vibrational analysis and chemical kinetics, *J. Chem. Inf. Model.* **50**(9) (2010) 1736–1750; https://doi.org/10.1021/ci100099g
47. A. Amić and D. Mastiľák Cagardová, DFT study of the direct radical scavenging potency of two natural catecholic compounds, *Int. J. Mol. Sci.* **23**(22) (2022) Article ID 14497 (15 pages); https://doi.org/10.3390/ijms232214497
48. F. A. M. Silva, F. Borges, C. Guimarães, J. L. F. C. Lima, C. Matos and S. Reis, Phenolic acids and derivatives: Studies on the relationship among structure, radical scavenging activity, and physicochemical parameters, *J. Agric. Food Chem.* **48**(6) (2000) 2122–2126; https://doi.org/10.1021/jf9913110
49. R. P. Bell, *The Tunnel Effect in Chemistry*, Chapman and Hall, London 1980.
50. A. Kohen, *Kinetic Isotope Effects as Probes for Hydrogen Tunneling in Enzyme Catalysis*, in *Isotope Effects in Chemistry and Biology*, (Ed. A. Kohen and H. H. Limbach), Taylor & Francis, CRC Press, New York 2006, pp. 744–764.
51. I. Nakanishi, Y. Shoji, K. Ohkubo and S. Fukuzumi, Tunneling in the hydrogen-transfer reaction from a vitamin E analog to an inclusion complex of 2,2-diphenyl-1-picrylhydrazyl radical with

β-cyclodextrin in an aqueous buffer solution at ambient temperature, *Antioxidants* **10**(12) (2021) Article ID 1966 (6 pages); https://doi.org/10.3390/antiox10121966

52. I. Sajenko, V. Pilepić, C. Jakobušić Brala and S. Uršić, Solvent dependence of the kinetic isotope effect in the reaction of ascorbate with the 2,2,6,6-tetramethylpiperidine-1-oxyl radical: Tunnelling in a small molecule reaction, *J. Phys. Chem. A* **114**(10) (2010) 3423–3430; https://doi.org/10.1021/jp911086n
53. C. Jakobušić Brala, V. Pilepić, I. Sajenko, A. Karković and S. Uršić, Ions can move a proton-coupled electron-transfer reaction into tunneling regime, *Helv. Chim. Acta* **94**(9) (2011) 1718–1731; https://doi.org/10.1002/hlca.201100035
54. S. Mundra, J. Tits, E. Wieland and U. M. Angst, Aerobic and anaerobic oxidation of ferrous ions in near-neutral solutions, *Chemosphere* **335** (2023) Article ID 138955 (12 pages); https://doi.org/10.1016/j.chemosphere.2023.138955.
55. T. C. Genaro-Mattos, Â. Q. Maurício, D. Rettori, A. Alonso and M. Hermes-Lima, Antioxidant activity of caffeic acid against iron-induced free radical generation – a chemical approach, *PLoS ONE* **10**(6) (2015) e0129963 (12 pages); https://doi.org/10.1371/journal.pone.0129963.
56. A. Shao, L. Mao, M. Tang, Z.-Y. Yan, J. Shao, C.-H. Huang, Z.-G. Sheng and B.-Z. Zhu, Caffeic acid phenyl ester (CAPE) protects against iron-mediated cellular DNA damage through its strong iron-binding ability and high lipophilicity, *Antioxidants* **10**(5) (2021) Article ID 798 (20 pages); https://doi.org/10.3390/antiox10050798
57. P. Sestili, G. Diamantini, A. Bedini, L. Cerioni, I. Tommasini, G. Tarzia and O. Cantoni, Plant-derived phenolic compounds prevent the DNA single-strand breakage and cytotoxicity induced by *tert*-butylhydroperoxide via an iron-chelating mechanism, *Biochem. J.* **364**(1) (2002) 121–128.; https://doi.org/10.1042/bj3640121